Mannosylated Poly(ethylene oxide)-*b*-Poly(ϵ-caprolactone) Diblock Copolymers: Synthesis, Characterization, and Interaction with a Bacterial Lectin

Jutta Rieger,[‡,†,§] Francois Stoffelbach,[†] Di Cui,[‡] Anne Imberty,[‡] Emilie Lameignere,[‡] Jean-Luc Putaux,[‡] Robert Jérôme,[†] Christine Jérôme,[†] and Rachel Auzély-Velty*[,‡]

Centre de Recherches sur les Macromolécules Végétales (CERMAV-CNRS), BP53, 38041 Grenoble cedex 9, France (affiliated with Université Joseph Fourier, and member of the Institut de Chimie Moléculaire de Grenoble), and Center for Education and Research on Macromolecules (CERM), University of Liége, Sart-Tilman B6, B-4000 Liége, Belgium

Received March 27, 2007; Revised Manuscript Received June 15, 2007

A novel bioeliminable amphiphilic poly(ethylene oxide)-*b*-poly(ϵ-caprolactone) (PEO-*b*-PCL) diblock copolymer end-capped by a mannose residue was synthesized by sequential controlled polymerization of ethylene oxide and ϵ-caprolactone, followed by the coupling of a reactive mannose derivative to the PEO chain end. The anionic polymerization of ethylene oxide was first initiated by potassium 2-dimethylaminoethanolate. The ring-opening polymerization of ϵ-caprolactone was then initiated by the ω-hydroxy end-group of PEO previously converted into an Al alkoxide. Finally, the saccharidic end-group was attached by quaternization of the tertiary amine α-end-group of the PEO-*b*-PCL with a brominated mannose derivative. The copolymer was fully characterized in terms of chemical composition and purity by high-resolution NMR spectroscopy and size exclusion chromatography. Furthermore, measurements with a pendant drop tensiometer showed that both the mannosylated copolymer and the non-mannosylated counterpart significantly decreased the dichloromethane/water interfacial tension. Moreover, these amphiphilic copolymers formed monodisperse spherical micelles in water with an average diameter of ∼11 nm as measured by dynamic light scattering and cryo-transmission electron microscopy. The availability of mannose as a specific recognition site at the surface of the micelles was proved by isothermal titration microcalorimetry (ITC), using the BclA lectin (from *Burkholderia cenocepacia*), which interacts selectively with α-D-mannopyranoside derivatives. The thermodynamic parameters of the lectin/mannose interaction were extracted from the ITC data. These colloidal systems have great potential for drug targeting and vaccine delivery systems.

Introduction

Cell surface carbohydrates from glycoproteins and glycolipids play a key role as recognition sites between cells, but also between cells and microorganisms. The recognition mechanisms are based on specific interactions between the saccharide residues and protein receptors, the so-called "lectins".[1] Thus, numerous polymeric materials carrying saccharide moieties, such as linear polymers,[2,3] dendrimers,[4−6] polymer micelles,[7] and nanoparticles,[8] have been developed for analytical, diagnostic, and therapeutic purposes. It was shown that materials that contain saccharides in a polyvalent array can exhibit enhanced binding capacity with lectins (due to "the cluster glycoside effect"), while the monomeric carbohydrate derivatives exhibit only weak affinity to the same lectins.[9−12] Such materials are promising carrier systems in drug delivery because of the specific cellular targeting of the drugs via the membrane lectins, which often participate in the internalization of their ligands.[13] It should be noted that the binding of a sugar to a specific glycoreceptor closely depends on the configuration of the anomeric (C-1) carbon of the sugar. Therefore, carbohydrates should be incorporated stereoselectively in the polymers in order to interact efficiently with the receptor.

Interestingly, dendritic cells express a variety of lectins at their surface, including specific receptors for mannose. These cells capture, process, and display antigens to native T cells, which initiate the cellular immune response.[14] They have thus been identified as a potent target for vaccine delivery in order to initiate adaptive immune responses.[15] The possible specific targeting of dendritic cells makes mannose-coated colloids attractive delivery systems for vaccines.

The purpose of this study was the synthesis of an amphiphilic biodegradable/bioresorbable mannosylated diblock copolymer as a novel precursor of colloidal (drug) delivery systems. This copolymer consists of a hydrophobic, biodegradable poly(ϵ-caprolactone) (PCL) segment and a hydrophilic, bioeliminable poly(ethylene oxide) (PEO) segment, end-capped by a reactive mannose derivative on the PEO side. The amphiphilic and self-assembling properties of the diblock copolymer were studied together with its recognition by a mannose-specific bacterial lectin.

Experimental Section

Materials. Polymerizations were carried out under dry and oxygen-free argon using standard Schlenk techniques. ϵ-Caprolactone (ϵ-CL) (Aldrich, 99%) was dried over calcium hydride under stirring at room temperature for 48 h and purified by vacuum distillation just before

* Corresponding author. E-mail: rachel.auzely@cermav.cnrs.fr; fax: +33 476 54 72 03.

‡ Centre de Recherches sur les Macromolécules Végétales.

† University of Liége.

§ Present address: Laboratoire de Chimie des Polymères, Université Pierre et Marie Curie-Paris 6, CNRS-UMR 7610, 4 Place Jussieu, 75252 Paris Cedex 05, France.

10.1021/bm070342y CCC: $37.00
Published on Web 08/17/2007

use. Toluene and tetrahydrofuran (THF) were purified by distillation under nitrogen after drying over sodium benzophenone complex. Dichloromethane (CH_2Cl_2) and pyridine were dried by refluxing over calcium hydride for at least 48 h and distilled prior to use. Acetic acid (AcOH), boron trifluoride diethyl etherate ($BF_3{\cdot}OEt_2$) (Fluka, 96%), 2-bromoethanol (Fluka, >95%), 3,3-diethoxy-1-propanol (Aldrich, 98%), diethyl ether (Vel), 2-dimethylamino ethanol (Aldrich, 99.5%), *N*,*N*-dimethylformamide (DMF) (Fluka, over molecular sieve, >99.8%), ethylene oxide (EO) (Messer), 1-*O*-methyl-α-D-mannopyranoside (Sigma, >99%), D-(+)-mannose (Sigma, >99%), methanol (Fluka, over molecular sieve, >99.5%), 2-propanol (^{i}PrOH), toluene (Fluka), and triethylaluminum ($AlEt_3$) (Fluka, 1.9 M in toluene) were used as received. Milli-Q water was used for all the experiments.

NMR Spectroscopy. ^{1}H NMR and ^{13}C NMR experiments were performed at 25 °C using a Bruker DRX400 spectrometer operating at 400 and 100 MHz, respectively. Chemical shifts (δ in ppm) were reported with respect to external tetramethylsilane (TMS = 0 ppm), and calibration was performed using the signal of the residual protons of the solvent as a secondary reference. Deuterium oxide (D_2O) and deuterated chloroform ($CDCl_3$) were purchased from SDS (Vitry, France). Detailed conditions are given in the figure captions.

Mass Spectrometry (MS). Electrospray mass spectra were recorded in the positive mode on a ZabSpec time-of-flight (Micromass, U.K.) mass spectrometer. The mannose derivatives were dissolved in methanol and injected into the electrospray ion source. The capillary voltage was set to 4 kV. Poly(ethylene glycol) standards were used for external calibration.

Size Exclusion Chromatography (SEC). The number-average molecular weight (M_n) and polydispersity (M_w/M_n) were determined by SEC at 45 °C. The chromatograph was equipped with a refractive index detector and two polystyrene gel columns (columns HP PL gel 5 μm, porosity: 10^2, 10^3, 10^4, and 10^5Å, Polymer Laboratories) that were eluted by THF or DMF at a flow rate of 1 mL/min. The columns were calibrated with polystyrene and PEO standards (Polymer Laboratories), respectively.

Dynamic Light Scattering (DLS). The size and size distribution of the micelles were determined by DLS with an ALV5000 digital correlator in combination with an ALV goniometer and an ALV-SIPC photomultiplier. The incident light source was an ionized argon laser (Spectra Physics 2016) emitting at $\lambda = 488$ nm. Micellar solutions at 25 °C were filtered through Millex-GS filters (porosity 0.22 μm) prior to measurements. The intensity autocorrelation functions ($g_2(t,\theta)$) measured at a given angle (θ) were analyzed with the REPES routine[16] according to a continuous distribution of relaxation times. The average relaxation times components were q^2 dependent in the investigated angular range (from 30 to 140°), such that diffusive motions were probed. The term q is the wave vector defined as $q = 4\pi n/(\lambda \sin(\theta/2))$, where n is the refractive index of the solvent.

Interfacial Tension Measurements. The CH_2Cl_2/H_2O interfacial tension was measured at 20 °C with a drop tensiometer (TRACKER, ITConcept, Longessaigne, France) equipped with a Bioblock Scientific Polystat CC2.[17] Dichloromethane solutions of the copolymers of different concentrations were prepared with CH_2Cl_2 previously saturated with Milli-Q water (mixing for 24 h). A drop of constant volume (5−10 μL) of each solution was formed in water (6 mL, preliminarily saturated with CH_2Cl_2), and the dynamic interfacial tension $\gamma(t)$ was determined by analyzing the axial symmetric shape (Laplacian profile) of the pendant drop in Milli-Q water.

Cryo-Transmission Electron Microscopy (Cryo-TEM). The morphology and size of the micelles were determined from cryo-TEM images. According to protocols reported elsewhere,[18−20] thin liquid films of nanoparticle suspensions (at 0.1 wt % solid content) were prepared on NetMesh (Pelco, U.S.A.) "lacey" carbon membranes and quench-frozen in liquid ethane. Once mounted in a Gatan 626 cryo-holder cooled with liquid nitrogen, the samples were transferred to a microscope and observed at low temperature (−180 °C). Images were recorded on Kodak SO163 film, using a Philips CM200 "Cryo" electron microscope operating at 80 kV.

Isothermal Titration Calorimetry (ITC). The specific recognition properties of the mannosylated micelles were examined by ITC using the BclA lectin produced in *E. coli*. BclA is a bacterial lectin from *Burkholderia cenocepacia* that shows strong sequence similarity with the well-characterized PA-IIL lectin from *Pseudomonas aeruginosa*[21] and binds α-D-mannopyranose (αMan) with high affinity ($K_{a\ (BclA/\alpha MeMan)} = 3.6 \times 10^5\ M^{-1}$),[22] much more strongly than Concanavalin A (ConA) ($K_{a\ (ConA/\alpha MeMan)} = 8.2 \times 10^3\ M^{-1}$).[23] Experiments were carried on a Microcal VP−ITC titration microcalorimeter (Northampton, MA). All titrations were made in 0.1 M tris(hydroxymethyl)aminomethane hydrochloride (Tris-HCl) buffer, pH 7.5, with 0.03 mM $CaCl_2$ at 25 °C. The reaction cell ($V = 1.4478$ mL) contained either (a) a solution of BclA lectin ([monomer] = 0.04 mM) or (b) the micellar solution ($[Mannose]_{exp} = 0.1$ mM). A series of 30 injections of 10 μL from the computer-controlled 300-μL microsyringe at an interval of 5 min of (a) the micellar solution ($[Mannose]_{theo} = 0.5$ mM) or (b) the solution of BclA ([monomer] = 2 mM) were performed into the receptor solution while stirring at 297 rpm at 25 °C. The raw experimental data were reported as the amount of heat produced after each injection of ligand as a function of time. The amount of heat produced per injection was calculated by integrating the area under the individual peaks by the instrument software, while taking into account the heat of dilution. The experimental data were fitted to a theoretical titration curve using the instrument software (ORIGIN software (Microcal)), refining the enthalpy change (in kJ/mol), ΔH, the association constant (in L/mol), K_a, and the stoichiometry of the interaction (number of binding sites per receptor), n.[24] Calculations were performed using the "one set of binding sites" model.

Synthesis. Synthesis of the mannose derivatives was monitored by thin-layer chromatography (TLC) on a precoated plate of silica gel 60 F_{254} (layer thickness 0.2 mm; E. Merck), with detection by UV absorption and/or by charring with a 5% (v/v) ethanolic solution of sulfuric acid. Flash column chromatography was performed on silica gel (Merck Gerduran SI 60, 40−63) with the appropriate eluant. The purity of the compounds was determined by ^{1}H NMR spectroscopy and MS, respectively. When no trace of byproducts was observed by NMR and MS, the products were reported as ">95%" pure (no trace by NMR) and ">99% pure" (no trace by MS).

*1,2,3,4,6-Penta-O-acetyl-D-mannopyranose (**1**).* α-D-Mannose pentaacetate was synthesized as commonly reported in the literature.[25] The peracetylated sugar was dried by three azeotropic distillations of toluene just before the next synthesis step.

*2-Bromoethyl-2,3,4,6-tetra-O-acetyl-α-D-mannopyranoside (ManOAc-Br) (**2**).* To a solution of 5.00 g of dried acetylated sugar **1** (0.013 mol) and 1.84 mL of 2-bromoethanol (0.017 mol) in 30 mL of dry CH_2Cl_2, 11.0 mL of $BF_3{\cdot}OEt_2$ (0.090 mol) were added dropwise at 0 °C over a period of 30 min under nitrogen. The progress of the reaction was followed by TLC (7:3 ethyl acetate/ cyclohexane). After 6 h of stirring at room temperature under nitrogen, the reaction mixture was slowly added to 40 mL of ice-cooled water. The aqueous phase was extracted with 20 mL of CH_2Cl_2. The combined organic phases were washed with a saturated aqueous solution of $NaHCO_3$ (20 mL), H_2O (2 × 5 mL), and dried (Na_2SO_4). The solvent was evaporated under vacuum at room temperature, and the crude product was purified by flash chromatography over silica (1:2 ethyl acetate/cyclohexane), to give 4.01 g (8.83 mmol) of **2** as a white crystalline solid.

Yield: 69%; purity: >99%; TLC: $R_f = 0.75$ (6.5:3.5 EtOAc/cyclohexane) (H_2SO_4).

^{1}H NMR ($CDCl_3$, 400 MHz) δ (ppm): 3.52 (t, *2H*, C*H*$_2$Br), 3.88 (m, *1H*, C*H*HCH$_2$Br), 3.98 (m, *1H*, CH*H*CH$_2$Br), 4.12−4.18 (m, *2H*, H-5, H-6a), 4.29 (m, *1H*, H-6b), 4.88 (d, *1H*, H-1), 5.26 − 5.38 (m, *3H*, H-2, H-4, H-3). ^{13}C NMR ($CDCl_3$, 100 MHz) δ (ppm): 21.98, 22.03, 22.07, 22.19 (4×*C*H$_3$COO), 30.09 (OCH$_2$*C*H$_2$Br), 63.76 (C-6), 67.28 (C-4), 69.78, 70.19, 70.32, 70.69 (*C*H$_2$CH$_2$Br, C-5, C-3, C-2), 99.08 (C-1), 171.01, 171.14, 171.32, 171.99 (4 × CH$_3$*C*OO). ESI-

Scheme 1. Synthetic Pathway to the Mannosylated Amphiphilic Copolymer **6**

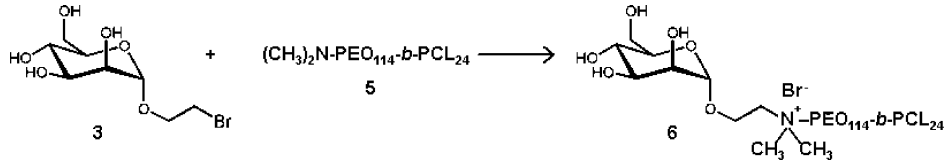

Scheme 2. Synthesis of the 2-Bromoethyl-α-D-mannopyranoside **3**

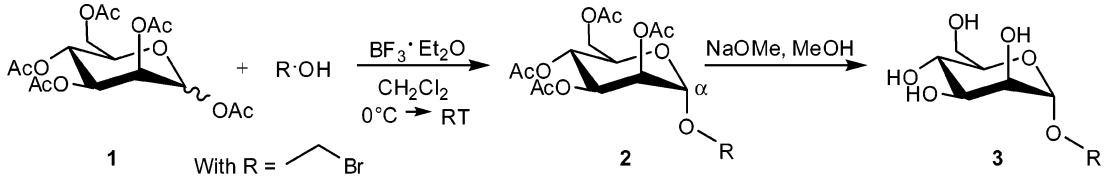

HRMS: $C_{16}H_{23}O_{10}BrNa$ $[M+Na]^+$, M_{theor} *m/z*: 477.03723, $M_{ESI-HRMS}$ *m/z*: 477.0358.

2-Bromoethyl-α-D-mannopyranoside (ManOH-Br) (3). Compound **2** (1.10 g, 2.41 mmol) was dissolved in 25 mL of dry methanol, and 1.6 mL of 0.82 M NaOMe (1.3 mmol) were added under nitrogen. After 35 h of stirring at room temperature, the solution was neutralized with an Amberlite IR-120 (H^+) resin and filtered off. Solvent was evaporated to give 0.69 g (2.41 mmol) of **3** as a waxy solid.

Yield: 100%; purity: >99%; TLC: R_f = 0.02 (7:3 EtOAc/cyclohexane) (H_2SO_4).

^{1}H NMR (D_2O, 400 MHz) δ (ppm): 3.52−3.60 (m, *3H*, CHHC*H*$_2$-Br, H-4), 3.66−3.95 (m, *7H*, C*HH*CH$_2$Br, H-2, H-3, H-5, H-6a, H-6b), 4.84 (d, *1H*, H-1). ^{13}C NMR (D_2O, 100 MHz) δ (ppm): 32.6 (C_t, OCH$_2$*C*H$_2$Br), 62.2 (C-6), 67.8 (C-4), 68.8, 71.2, 71.8, 74.2 (CH$_2$CH$_2$-Br, C-5, C-3, C-2), 101.0 (C-1). ESI-HRMS: $C_8H_{15}O_6BrNa$ $[M+Na]^+$, M_{theor} *m/z*: 308.99497, $M_{ESI-HRMS}$ *m/z*: 308.9941; $C_8H_{15}O_6BrK$ $[M+K]^+$, M_{theor} *m/z*: 324.96891, $M_{ESI-RHMS}$ *m/z*: 324.9674.

α-N,N-Dimethylaminoethyl Poly(ethylene oxide) (Me$_2$N-PEO-OH) (4). In a flame-dried and argon-purged flask, 200 mL of anhydrous THF, 1.2 mL of *N*,*N*-dimethylaminoethanol (12 mmol) and 15 mL of a potassium naphthalene/THF solution (0.8 M) were added under argon. After vigorous stirring at room temperature for 15 min, the mixture was added into a 500 mL Parr reactor followed by 60 g of EO (1.36 mol). After 19 h of polymerization at 30 °C, 2-propanol was added, and polymer **4** was precipitated by an excess of diethyl ether and vacuum-dried at 30 °C.

Yield: 95%; $M_{n,NMR}$ = 5470 g/mol; M_w/M_n (SEC) = 1.06; end functionality > 95%.

^{1}H NMR ($CDCl_3$, 400 MHz) δ (ppm): 2.22 (s, *6H*, C*H*$_3$−N), 2.47 (m, *2H*, CH$_3$−N−C*H*$_2$), 3.62 (m, *4H*, O−C*H*$_2$−C*H*$_2$−O−).

α-N,N-Dimethylaminoethyl Poly(ethylene oxide)-b-Poly(ϵ-caprolactone) (Me$_2$N-PEO-b-PCL-OH) (5). In a flame-dried and argon-purged flask, compound **4** (Me$_2$N-PEO-OH) (1.6 g, 0.3 mmol) was dried by azeotropic distillation with toluene (3 × 10 mL). Then 3 mL of dry toluene, one drop of pyridine, and $AlEt_3$ (0.25 mL, 1.9 M, 0.48 mmol) were added. After 20 min at room temperature, 3 mL of CH_2Cl_2 and 0.8 mL of ϵ-CL (7.2 mmol) were added. After 36 h, the polymerization was stopped by an excess of acetic acid solution (1 M in water), and polymer **5** was recovered by precipitation within a 10-fold excess of heptane and vacuum-dried.

For the preparation of micelles, the polymer was dissolved in acetone, filtered through a 0.2 μm Millex LG (Millipore), and dried in a vacuum.

Yield: 95%; $M_{n,NMR}$ = 8300 g/mol; M_w/M_n (SEC) = 1.10; end functionality > 95%.

^{1}H NMR ($CDCl_3$, 400 MHz) δ (ppm): 1.35 (m, *2H*, CH$_2$−C*H*$_2$−CH$_2$), 1.65 (m, *4H*, C*H*$_2$−CH$_2$-C*H*$_2$), 2.27 (s, *6H*, C*H*$_3$−N), 2.30 (m, *2H*, C*H*$_2$−COO), 2.51 (t, *2H*, CH$_3$−N−C*H*$_2$), 3.63 (m, *4H*, O−C*H*$_2$−C*H*$_2$−O−), 4.05 (t, *2H*, COO−C*H*$_2$), 4.22 (t, *2H*, PCL−COO−C*H*$_2$−CH$_2$−O−PEO).

PEO-b-PCL End-Capped by a Mannose Residue via Quaternization (6). A 0.46 g portion of compound **5** (0.06 mmol) was dissolved in 10 mL of dry DMF. Then, 0.28 g of **3** (0.98 mmol) dissolved in 10 mL of DMF was added. After 50 h of stirring under nitrogen at 70 °C, the reaction mixture was concentrated to 5 mL by partial evaporation of the solvent. Then, 10 mL of water was added, and the mixture was introduced in a dialysis membrane (cutoff 3500) and then dialyzed against Milli-Q water for 48 h. The polymer was recovered by freeze-drying as a white solid (0.45 g).

For the preparation of micelles, compound **6** was dissolved in acetone, filtered through a 0.2 μm Millex LG (Millipore), and dried in a vacuum. It was stored at −20 °C.

Yield: 96%; $M_{n,NMR}$ = 8500 g/mol; M_w/M_n (SEC) = 1.19; end-group functionalization ~ 80%.

^{1}H NMR ($CDCl_3$, 400 MHz) δ (ppm): 1.35 (m, *2H*, CH$_2$−C*H*$_2$−CH$_2$), 1.65 (m, *4H*, C*H*$_2$−CH$_2$−C*H*$_2$), 2.30 (m, *2H*, C*H*$_2$−COO), 3.32 (s, *6H*, C*H*$_3$−N), 3.45−4.05 (m, *10H*, mannose), 3.63 (m, *4H*, O−C*H*$_2$−C*H*$_2$−O−), 4.05 (t, *2H*, COO−C*H*$_2$), 4.22 (t, *2H*, PCL−COO−C*H*$_2$−C*H*$_2$−O−PEO), 4.95 (s, *1H*, H-1, mannose).

Preparation of Micellar Solutions. Typically, 50 mg of amphiphilic copolymer was dissolved in 3 mL of THF (c = 16.6 mg/mL). After complete dissolution of the copolymer, 3 mL of aqueous Tris buffer solution was added dropwise. The mixture was dialyzed (pre-swollen semipermeable membrane: cutoff 3500) for 12 h against Tris buffer that was regularly replaced.

The content of mannose in the micellar solution was determined by acidic hydrolysis of the copolymer. Thus, the micellar solution (1 mL) was heated under acidic conditions (2 M trifluoroacetic acid (0.5 mL) for 4 h at 100 °C). Mannose was quantitatively analyzed after conversion to mannitol acetate by gas chromatography (Hewlett-Packard 5890) and fitted with a flame-ionization detector and a SP2380 column (30 m × 0.53 mm i.d.) using N_2 as a gas carrier.

Results and Discussion

Synthesis of the Targeted Mannosylated Amphiphilic Copolymer. As illustrated in Scheme 1, the strategy for the synthesis of the mannosylated amphiphilic PEO-*b*-PCL diblock copolymer relied on a quaternization reaction between a brominated mannose derivative **3** and a PEO-*b*-PCL diblock copolymer end-capped by a tertiary amine **5**.

The brominated mannose derivative **3** was synthesized by glycosylation of 2-bromoethanol by penta-*O*-acetyl-*β*-D-mannopyranoside **1**,[25] in the presence of an excess of boron trifluoride etherate. The α-mannoside **2** was stereoselectively formed (Scheme 2). After purification by flash chromatography, compound **2** (69% yield) was deacetylated under Zemplén conditions to give quantitatively 2-bromoethyl-α-D-mannopy-

Scheme 3. Synthetic Pathway to Amphiphilic PEO-*b*-PCL Copolymers α-End-Capped by a Tertiary Amine

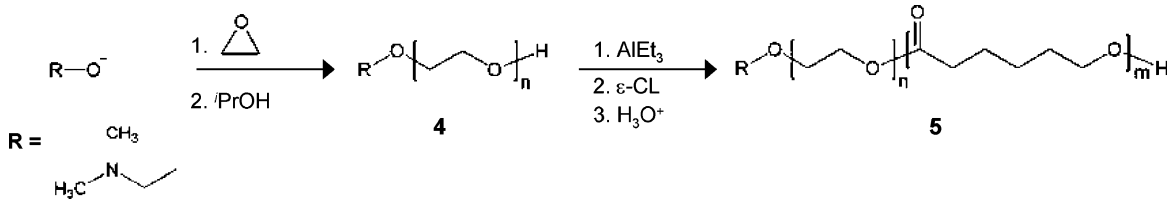

Table 1. Macromolecular Characteristics of α-*N*,*N*-dimethylaminoethyl PEO **4**, α-*N*,*N*-dimethylaminoethyl PEO-*b*-PCL **5,** and the Mannosylated Copolymer **6**

#	polymer	$M_{n,theor}$	$M_{n,NMR}$	$M_{n,SEC}$	M_w/M_n[e]
4	Me_2N−PEO-OH	5090[a]	5470	5050[e]	1.06
5	Me_2N−PEO-*b*-PCL	8210[b]	8300[d]	7100[e]	1.10
6	(Mannose)Me_2N^+− PEO-*b*-PCL	8500[c]	8500	7440[e]	1.19

[a] $M_{n,theor}$ = [[EO]$_0$/ROH × MW_{EO}] + MW (*N*,*N*-dimethylaminoethanol) at 100% of conversion. [b] $M_{n,theor}$ = [[ε-CL]$_0$/[Me_2N−PEO-OH] × $MW_{ε-CL}$] + 5470. [c] $M_{n,theor}$ = MW(1-*O*-ethyl-α-D-mannoside) + 8300. [d] $M_{n,NMR}$ = DP(PCL) × $MW_{ε-CL}$ + 5470; $M_{n,NMR}$ is the number average molecular weight determined by ^{1}H NMR spectroscopy. [e] As determined by SEC in THF calibrated by PEO standards.

roside **3**. The chemical structure of **3** was confirmed by ^{1}H NMR and high-resolution electrospray MS.

The PEO-*b*-PCL copolymer was synthesized by controlled polymerization techniques, in order to tune the molecular weight of the two blocks and to favor a narrow molecular weight distribution.[26] Indeed, for the envisioned PEO-*b*-PCL copolymers to self-assemble into colloidal delivery systems in water, it is essential to precisely control their hydrophilic−lipophilic balance. The hydrophilic PEO block was synthesized first by the "living" anionic polymerization of EO, initiated by potassium *N*,*N*-dimethylaminoethanolate (Scheme 3).

The number average molecular weight (M_n) of the PEO block **4** was determined by ^{1}H NMR from the relative intensity of the proton signals of the PEO chain at 3.62 ppm ($I_{3.62ppm}/4$) and the methyl groups (CH_3N) of the tertiary amine end-group at 2.22 ppm ($I_{2.22ppm}/6$) (Table 1). The polymer **4** was eluted in a single and narrow fraction by SEC (data not shown). The molecular weight determined by NMR and SEC (using a PEO standard) agreed with the value predicted by the monomer/initiator ratio and the monomer conversion (see Table 1, entry 4).

In a second step, the ω-hydroxyl group of the PEO chain was reacted with $AlEt_3$ and converted into an Al alkoxide, which is the actual initiator of the ring-opening polymerization of ε-CL.[27] The length of the PCL block was controlled by the ε-CL over PEO-Al alkoxide molar ratio. The PEO-*b*-PCL diblock copolymer **5** was isolated by precipitation in heptane and characterized by SEC and ^{1}H NMR. The size exclusion chromatogram of the copolymer was narrow (M_w/M_n = 1.10) and unimodal (cf. Supporting Information Figure S1, trace A), indicating the complete initiation of the polymerization of ε-CL by the PEO macroinitiator. The average number molecular weight (M_n) of the PCL block could be determined by ^{1}H NMR spectroscopy (cf. Supporting Information Figure S2). The M_n of the PCL segment was close to the theoretical value, consistent with polymerization control (see Table 1, entry 5).

The final step to the targeted mannosylated copolymer was the quaternization of the tertiary amine-functionalized copolymer by the brominated mannose derivative (Scheme 1). The same reaction was previously used to selectively and quantitatively convert poly(ε-caprolactone)-*co*-poly(γ-bromo-ε-caprolactone) chains into the corresponding pyridinium salts.[28−30] Depending on the copolymer composition, amphiphilic or water-soluble polyesters were prepared in good yields (90%) without degradation of the polyester.

Here, the mannose derivative **3** was covalently bonded to the tertiary amino end-group of the amphiphilic PEO-*b*-PCL copolymer **5** merely by heating the mixture of the two compounds in an appropriate solvent, without assistance of activating agents. For optimization of the reaction, the yield in ammonium salt was determined for different reaction conditions (solvent, bromide/tertiary amine molar ratio, and temperature; cf. Supporting Information Table S1).

Clearly, a large excess of 2-bromoethyl-α-D-mannopyrano side was needed. Moreover, high reaction temperature and long reaction time significantly improved the reaction yield. The best results were obtained within 5 h, in dry DMF at 70 °C, with a large excess of the brominated mannose-derivative (>15 molar equiv) compared to the tertiary amine end-groups (cf. Supporting Information Table S1, entry E). However, longer reaction times (5 days) did not improve the conversion of the quaternization, but led to the degradation of the polymer backbone. (cf. Supporting Information Table S1, entry F)

After reaction, the excess mannose was removed by dialysis against water for 48 h, and the purified product was recovered in good yield by freeze-drying. Figure 1 shows the ^{1}H NMR spectrum of copolymer **6** prepared in 50 h with an excess of 15 equiv of mannose at 70 °C in DMF (cf. Supporting Information Table S1, reaction conditions E).

^{1}H NMR spectroscopy allowed the determination of the degree of glycosylation and the successful elimination of excess mannose; compared to the spectrum of copolymer **5** before derivatization (cf. Supporting Information Figure S2), new resonances in the range of 3.4 to 5.0 ppm were observed, which are characteristic of the protons of the mannose moiety. The signal at 4.95 ppm can be attributed to the anomeric proton of mannose (H_1). Furthermore, the two peaks at 2.27 ppm (6H, CH_3−N) and at 2.51 ppm (2H, N−CH_2), characteristic of the tertiary amino end-group of PEO-*b*-PCL (**5**), disappeared, indicating the total conversion into ammonium salt. Moreover, a resonance observed at 3.32 ppm was found to be 6 times more intense than the anomeric proton H_1 of mannose. It was attributed to the methyl protons of the quaternary ammonium salt, in agreement with the chemical shift of the methyl protons of quaternary ammonium salts found in the literature.[31] The integrals ratio of 1:6 provides evidence for the complete removal of unreacted mannose.

Finally, the same copolymer **6** was analyzed by SEC to confirm that the polymer was not degraded upon quaternization. The chromatogram of the glycosylated polymer remains unimodal and narrow (cf. Supporting Information Figure S1, trace B), consistent with the absence of degradation and side reactions (M_w/M_n = 1.19).

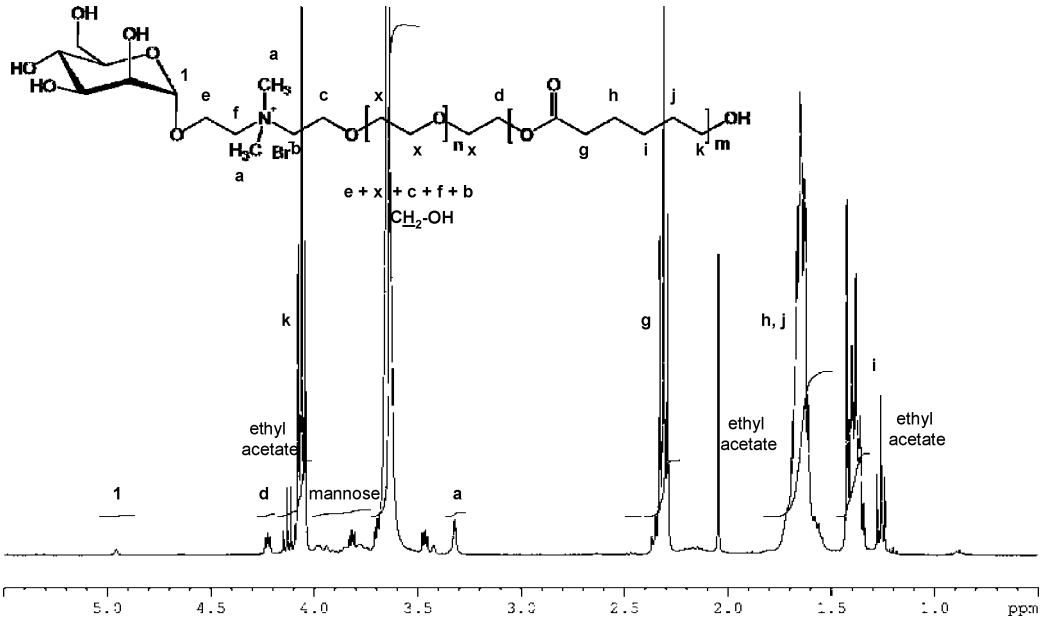

Figure 1. ^{1}H NMR spectrum (400 MHz, 25 °C, $CDCl_3$) of α-mannosylated PEO-*b*-PCL **6** from copolymer **5**.

In conclusion, the tertiary amino end-group of Me_2N-PEO-*b*-PCL was quaternized by brominated-mannose within good yields, without significant chain degradation and without the need of protection/deprotection chemistry.

Amphiphilic Properties of the (Glyco)polymers: Dynamic Interfacial Tension Measurements and Micelle Formation. The amphiphilic properties of the mannosylated copolymer **6** (Table 1) and the parent copolymer **5** (Table 1) were investigated using a drop tensiometer (TRACKER). As the copolymers were barely soluble in water, experiments were performed with solutions in dichloromethane (CH_2Cl_2). The CH_2Cl_2/water interfacial tension (γ) of different copolymer solutions was measured as a function of time. For pure CH_2Cl_2/H_2O (mutually saturated by H_2O and CH_2Cl_2, respectively), the interfacial tension was 28 mN/m and did not vary with time. Figure 2 shows the dynamic interfacial tension isotherms $\gamma(t)$ for solutions of copolymers **5** (Figure 2 A) and **6** (Figure 2 B) at different concentrations, C_S, in CH_2Cl_2.

As a rule, several steps of adsorption were observed with different characteristic relaxation times: the induction step (*lag stage* for $t < \tau_1$), the post-induction step (*post-lag stage* for $\tau_1 < t < \tau_2$), and the final step ($t > \tau_2$). As shown in Figure 2, the *lag time* τ_1 is well defined for relatively low concentrations C_S ($< 5 \times 10^{-3}$ mg/mL), with a slow decrease of $\gamma(t)$ (curves 6, 5, and 4) at the beginning of the adsorption process. This induction time corresponds to the diffusion of the macromolecules from the bulk to the interface. Usually, when at the interface, macromolecules, such as polysoaps and proteins,[32−34] unfold and may adsorb irreversibly by anchoring their hydrophilic part into the polar phase. The *post-lag stage* of adsorption is characterized by a fast decrease in the interfacial tension ($d\gamma/dt$). During this period, the first layer adsorbed at $t < \tau_1$ is "compacted" by newly arriving polymer chains, which penetrate the layer of adsorbed molecules. At the end of the *post-lag stage*, the adsorption layer starts to act as a repulsive barrier against newly arriving macromolecules, as manifested by a remarkable decrease in $d\gamma/dt$ beyond time τ_2. Figure 2 indicates that the mannosylated copolymer **6** has a higher interfacial activity than copolymer **5**. This is confirmed in Figure 3, where the interfacial tension at an aging time of 1000 s is plotted as a function of the copolymer concentration.

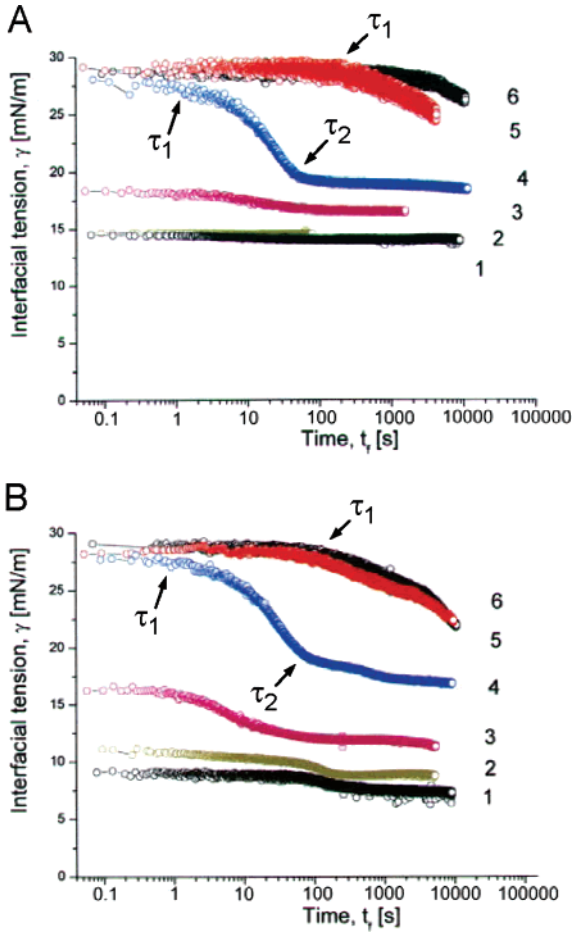

Figure 2. Kinetic curves for (A) copolymer **5**, Me_2N-PEO-*b*-PCL in CH_2Cl_2 at different concentrations C_S: (1) 1; (2) 0.5; (3) 5×10^{-2}; (4) 5×10^{-3}; (5) 5×10^{-4}; and (6) 5×10^{-6} mg/mL, and (B) copolymer **6**, (Mannose)Me_2N^+-PEO-*b*-PCL, Br^- in CH_2Cl_2 at (1) 5; (2) 0.5; (3) 5×10^{-2}; (4) 5×10^{-3}; (5) 5×10^{-4}; and (6) 5×10^{-6} mg/mL.

Both diblock copolymers **5** and **6** decrease the oil−water interfacial tension γ efficiently. At the same copolymer concentration in CH_2Cl_2, the quaternized copolymer **6** (bearing the mannose moiety) is, however, more effective. It must be noted

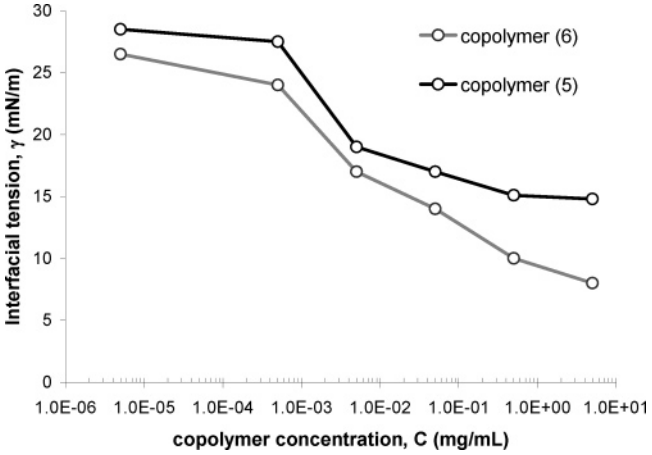

Figure 3. Adsorption isotherms of the interfacial tension γ at the H_2O/CH_2Cl_2 interface for copolymer **5** and its mannosylated counterpart **6**, measured at an aging time of 10^3 s.

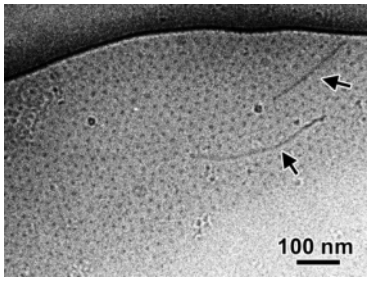

Figure 4. Cryo-TEM image of spherical micelles of the mannosylated copolymer **6** embedded in vitreous ice. The arrows indicate elongated objects that may correspond to cylindrical micelles.

that, at high concentrations ($c > 1$ mg/mL), the γ values are close to the limit of accuracy of the pendant drop method (drops fell down after a few minutes).

As the water solubility of the copolymers is extremely low, micelles from PEO-*b*-PCL diblock copolymers **5** and **6** were prepared by the dialysis method.[35,36] The concentration of the as-prepared micellar aqueous solutions was in the range of 10^{-3} to 10^{-4} M. The critical micelle concentration of PEO-*b*-PCL copolymers of very similar composition (M_n (PEO) = 5000 g/mol, M_n (PCL) = 2500 and 4000 g/mol)[37] has been reported in the range of 10^{-7} M, meaning that, at 10^{-4} M, the large majority of copolymer chains is present as micelles.

The size and shape of the micelles were analyzed by DLS and cryo-TEM. According to DLS analysis, the two copolymers formed monodisperse micelles with an average hydrodynamic radius R_H of ~11 nm. This value is of the same order of magnitude as the R_H reported for micelles of PEO-*b*-PLA[38] diblock copolymers (with M_n(PEO) = 5000, M_n(PLA) = 2000, and R_H = 9.5 nm)[38] and PEO-*b*-PCL[37,39] copolymers (e.g., for M_n(PEO) = 5000 and M_n(PCL) = 2500, and R_H = 11 nm).

The cryo-TEM image in Figure 4 shows micelles of the mannosylated copolymer **6** embedded in a thin film of vitreous ice. A homogeneous distribution of electron-dense particles is observed along with occasional elongated objects. The particles are not in contact, describing in some areas a more or less hexagonal pattern, with an average inter-particle distance of 24–26 nm. Moreover, the particles are at a distance of about 25 nm from the elongated objects. This suggests that the spherical micelles are made of an electron-dense core of PCL blocks surrounded by a more diffuse PEO corona. In the cryo-TEM images, the PCL cores would be at a distance of 25 nm from each other due to the steric repulsion of the PEO coronas. If

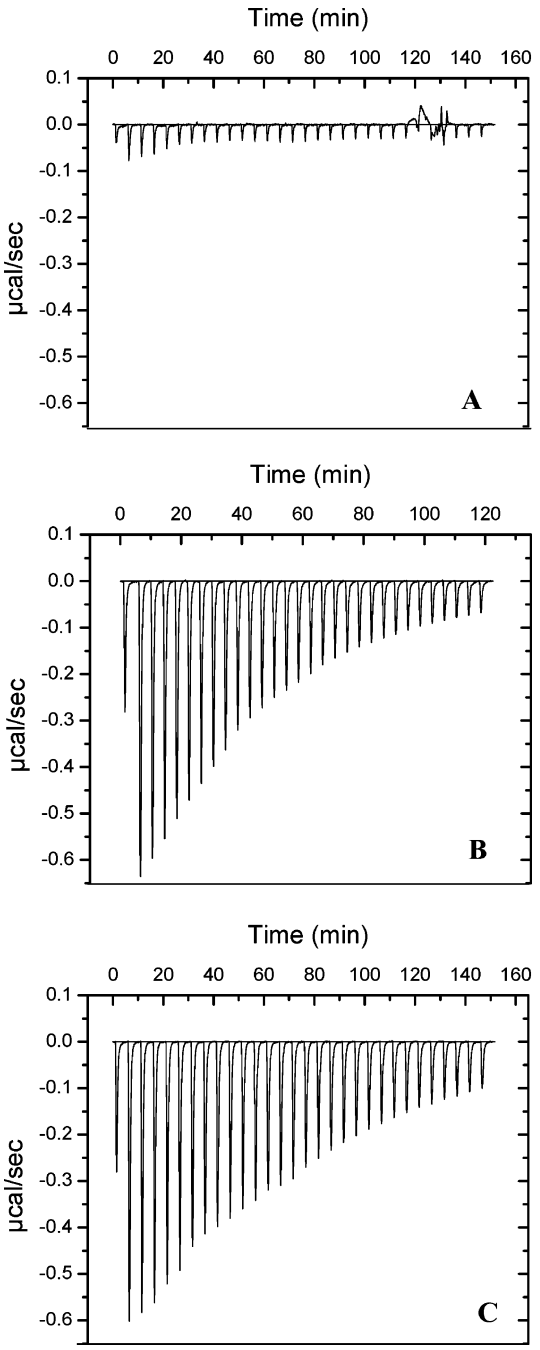

Figure 5. Calorimetric data for the titration of a solution of BclA lectin ([monomer] = 0.04 mM) with (A) a micellar solution of copolymer **5**, (B) a micellar solution of the mannosylated copolymer **6** ($[Mannose]_{theo}$ = 0.5 mM), and (C) a solution of αMeMan ([Mannose] = 0.5 mM), at 25 °C.

we assume that the particles are not interpenetrating, the radius of the micelles would be approximately 12 nm, in good agreement with the size measured by DLS. The occasionally observed elongated objects may correspond to cylindrical copolymer micelles with a diameter of about 25 nm.

Recognition of Surface-Exposed Mannose: Isothermal Titration Calorimetry. The availability of mannose as a specific recognition site at the surface of the micelles was assessed by ITC. This technique, which has been increasingly used for ligand binding studies during the past 15 years,[24] provides in a single measurement the binding constant, K_a, the enthalpy of binding, ΔH, and the stoichiometry, n, of the interaction. Although ConA is a commonly used lectin to demonstrate specific binding to mannose moieties, the recently

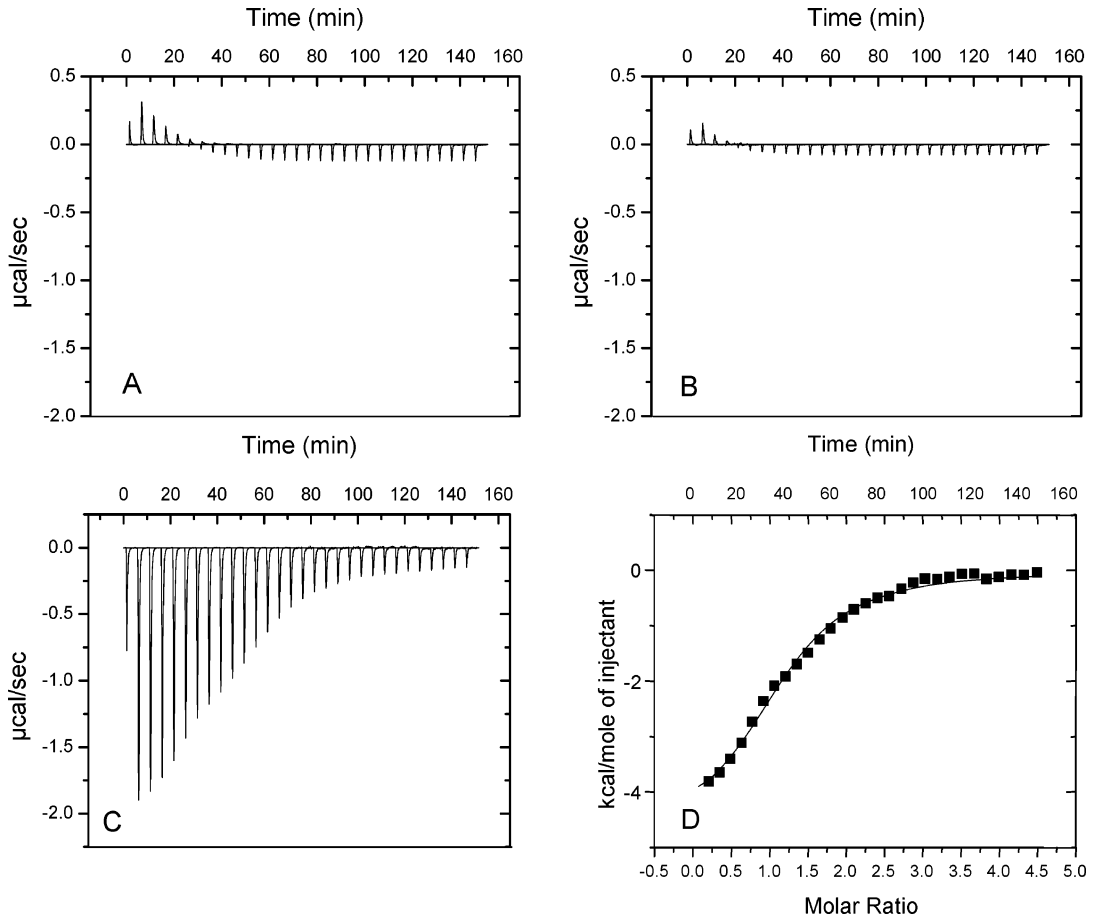

Figure 6. Calorimetric data for (A) the addition of a solution of BclA lectin ([Monomer] = 2 mM) to the micellar solution of the Me_2N-PEO-*b*-PCL copolymer **5**, (B) the addition of a solution of BclA lectin ([Monomer] = 2 mM) to Tris buffer solution, and (C) the titration of the micellar solution of mannosylated copolymer **6** ($[Mannose]_{theo}$ = 0.1 mM) by BclA lectin ([Monomer] = 2 mM) at 25 °C. (D) Integrated values of the peaks of thermogram C (after subtraction of thermogram A) (squares) and fit with the calculated curve (line).

characterized BclA lectin from *Burkholderia cenocepacia* was used in this study. Indeed, because of the low concentration of mannose in the micellar solutions ($[Mannose]_{theo}$ = 0.5 mM) herein prepared by the dialysis method and the relatively low association constant for the α-D-mannopyranoside derivatives (αMeMan) binding to ConA ($K_a = 8.2 \times 10^3\ M^{-1}$),[40] the heat evolved during titration was too small for an accurate characterization of the complex formation. In contrast, data could be collected with BclA, which binds αMan much more strongly than ConA ($K_a = 3.6 \times 10^5\ M^{-1}$). In a first step, ITC experiments were performed by adding the ligand (micelles with mannose) to the protein receptor in the microcalorimeter cell. Figure 5 compares the thermograms for the calorimetric titration of BclA at 25 °C with micellar solutions of copolymer **5**, mannosylated copolymer **6** ($[Man]_{theo}$ = 0.5 mM), and methyl α-D-mannopyranoside (αMeMan) ([Man] = 0.5 mM).

Compared to the titration with the non-mannosylated micelles, which yielded only small exothermic peaks (thermogram A), a substantial heat release was noted for the titration with the mannosylated micelles (thermogram B). The magnitude of this effect decreased progressively with the progress of the titration, which corresponds to the classically observed increase of occupancy of the receptor sites, similarly to the titration with free αMeMan (thermogram C). Thus, comparison of the thermograms of Figure 5 provides evidence for the selective interaction between mannose at the surface of the micelles and BclA. Furthermore, the similarity observed between thermograms B and C for the injection of similar amounts of mannose residues, strongly suggests that most of the mannose moieties in the micellar assemblies are available for complexation with BclA. In the case of the non-mannosylated micelles (thermogram A), the small heat release can be attributed to the dilution of the micellar solution. Nevertheless, the low concentrations of mannose and lectin used for the titration experiments did not allow the thermodynamic parameters for the mannose binding to BclA to be determined accurately.

Thus, in a second step, reverse titration was carried out. The micellar solution was titrated with the solution of the lectin, such that higher concentrations of ligand and receptor were used, making possible a more reliable determination of the calorimetric parameters. The thermograms for the titration of the mannosylated micelles by BclA (thermogram C), for the addition of BclA to the neat buffer solution (thermogram B), and for the addition of BclA to the Me_2N-PEO-*b*-PCL micelles (thermogram A) are shown in Figure 6. Thermograms A and B are very similar and consistent with the heat of dilution of lectin in the buffer containing micelles or not. Compared to the low endothermic signals in thermograms A and B, a strong exothermic effect is observed in thermogram C as result of the mannose complexation. The very low heat release observed for the last injections indicates that the complexation of mannose at the surface of the micelles is quasi complete. The thermodynamic parameters were extracted from the ITC data on the basis of the simplest model of binding that assumes that individual saccharides bind to individual discrete binding sites in a non-cooperative fashion. For this purpose, the effect of the lectin dilution in the micellar solution (no mannose involved) was taken into account, and thermogram A was subtracted from

Table 2. Thermodynamic Parameters Calculated from ITC[a]

compound	[αMeMan] (mM)	[BclA monomer] (mM)	$K_a \times 10^{-4}$ (M^{-1})	ΔH (kJ/mol)	$T\Delta S$ (kJ/mol)	n (Man: lectin)
αMeMan	3	0.3	36.4 (±1)	−23 (±0.4)	8.8 (±0.3)	0.83 (±0.11)
micelles of copolymer **6**	0.1[b]	2	3.9 (±0.4)	−20 (±0.7)	6.2 (±0.7)	1.18 (±0.03)

[a] Reported values are the mean of at least two experiments. Deviations reported in the fitting procedures are indicated in parenthesis. [b] Concentration of mannose determined by gas chromatography.

thermogram C as reported in Figure 6D. The goodness of fit between the titration data and the calculated curve validates the one-site model (Figure 6D). Table 2 compares the thermodynamic parameters calculated for the complex formation between BclA and free αMeMan, and between BclA and mannose at the surface of the micelles.

ΔH is comparable for the interaction of BclA with free mannose and micelle-bound mannose, consistent with a similar mechanism of binding, although a small loss of enthalpy is observed when the mannose residue is attached on the micelles. The entropy contribution is favorable for both ligands, which is unusual for protein−carbohydrate interactions[23] but was previously reported for this particular family of calcium-dependent bacterial lectins.[41] The fixation of mannose to the micelles results in a less favorable entropy term for binding to BclA. As the result of both enthalpy and entropy loss, the affinity constant of BclA for mannose at the surface of micelles by the lectin is 10 times weaker than that for free mannose. The entropy cost for fixing the ligand was previously reported for the complexation of hydrophobic guests by β-cyclodextrin, free and attached to polymer chains, respectively.[42] Moreover, the stoichiometry n is close to the theoretical value of 1 (one mannose complexed by one lectin monomer), which suggests that nearly all the mannose residues in the micellar solution are available for complexation by BclA.

In contrast to previously described micelles with galactose[43] or mannose[44] at their surface, no cooperative interaction between mannose and the BclA lectin is observed for the micellar aggregates in this study. Nevertheless, as previously pointed out,[5] the behavior of multivalent saccharide ligands is closely related to the assay used to evaluate them. Thus, enhancement in the apparent affinity reported in the literature for saccharide-functionalized micelles, on the basis of agglutination or affinity column inhibition assays, might result from entropically driven protein aggregation phenomena, which strongly depend on the molecular characteristics of the ligand and the protein concentration. Indeed, previous ITC experiments showed that enhanced apparent affinity might be explained by an enthalpy−entropy compensation.[5] Hence, a reduction in the binding enthalpy together with a large increase in entropy imposed by aggregation would lead to an overall increase in the binding constant. Therefore, it would be rash to compare the conclusions about ligand binding in this work with those reported in the literature.

Conclusions

A novel amphiphilic PEO-*b*-PCL diblock copolymer end-capped by a carbohydrate unit was synthesized by coupling a mannose derivative to the α-end-group of a PEO-*b*-PCL diblock copolymer. The length of each block was predetermined by the monomer-to-initiator molar ratio, because controlled polymerization techniques were used. The PEO block was first prepared by living anionic polymerization of EO initiated by potassium *N*,*N*-dimethylaminoethanolate. A tertiary amino α-end-group was accordingly made available for attaching a mannose moiety by quaternization with a brominated mannose derivative. The yield of the end-functionalization was high, and no chain degradation was observed. The interfacial activity of the diblock copolymer, mannosylated or not, was confirmed by measurements of the CH_2Cl_2/water interfacial tension. These amphiphilic polymers formed micelles of similar size, as confirmed by DLS and cryo-TEM. The interaction of the two types of micelles with a mannose-specific lectin (BclA) was investigated for the first time, to the best of our knowledge, by ITC. The thermograms unambiguously confirmed the bioavailability of mannose moieties of the "mannosylated" micelles. When targeting mannose-receptors at the surface of cells, the multivalency of the mannose presentation on the micelles will result in avidity phenomenon that will compensate the somewhat lower affinity observed in solution when comparing to free mannose. The next step of this study will focus on targeted drug delivery using these bioeliminable mannose-decorated micelles as carrier systems.

Acknowledgment. J.R., C.J., and R.J. are much indebted to the "Belgian Science Policy" for financial support in the frame of the "Interuniversity Attraction Poles Programme (IAP-PAI P6/27): Supramolecular Chemistry and Supramolecular Catalysis". J.R. was a recipient of a Marie Curie fellowship. C.J. is an Research Associate by the "Fonds National de la Recherche Scientifique" (FNRS). F.S., C.J., and R.J. also thank the FNRS for a grant to F.S. in the frame of the "SONS-EUROCORES" program. E.L. gratefully acknowledges the MENRT for her thesis grant at the CERMAV. Furthermore, the authors are very grateful to Gérard Chambat for technical support.

Supporting Information Available. SEC traces of α-*N*,*N*-dimethylaminoethyl PEO-*b*-PCL before and after glycosylation (copolymers **5** and **6**); ^{1}H NMR spectrum of α-*N*,*N*-dimethylaminoethyl PEO-*b*-PCL (copolymer **5**) and its discussion; optimization of the quaternization reaction: reaction conditions and yields. This material is available free of charge via the Internet at http://pubs.acs.org.

References and Notes

(1) Dwek, R. A. *Chem. Rev.* **1996**, *96*, 683−720.
(2) Narain, R.; Armes, S. P. *Biomacromolecules* **2003**, *4*, 1746−1758.
(3) Bes, L.; Angot, S. Limer, A.; Haddleton, D. M. *Macromolecules* **2003**, *36*, 2493−2499.
(4) Mangold, S. L.; Cloninger, M. J. *Org. Biomol. Chem.* **2006**, *4*, 2458−2465.
(5) Corbell, J. B.; Lundquist, J. J.; Toone, E. J. *Tetrahedron: Asymmetry* **2000**, *11*, 95−111.
(6) Fernandez-Megia, E.; Correa, J.; Riguera, R. *Biomacromolecules* **2006**, *7*, 3104−3111.
(7) You, L.-C.; Lu, F.-Z.; Li, Z.-C.; Zhang, W.; Li, F.-M. *Macromolecules* **2003**, *36*, 1−4.
(8) Cade, D.; Ramus, E.; Rinaudo, M.; Auzely-Velty, R.; Delair, T.; Hamaide, T. *Biomacromolecules* **2004**, *5*, 922−927.
(9) Nishimura, S. I.; Matsuoka, K.; Kurita, K. *Macromolecules* **1990**, *23*, 4182−4184.
(10) Nishimura, S. I.; Matsuoka, K.; Furuike, T.; Ishii, S.; Kurita, K.; Nishimura, K. M. *Macromolecules* **1991**, *24*, 4236−4241.
(11) Roy, R.; Pon, R. A.; Tropper, F. D.; Andersson, F. O. *J. Chem. Soc., Chem. Commun.* **1993**, 264−265.
(12) Zeng, X.; Murata, T.; Kawagishi, H.; Usui, T.; Kobayashi, K. *Carbohydr. Res.* **1998**, *312*, 209−217.

(13) Smart, J. D.; Nicholls, T. J.; Green, K. L.; Rogers, D. L.; Cook, J. D. *J. Pharm. Sci.* **2000**, *9*, 93−99.
(14) McGreal, E. P.; Miller, J. L.; Gordon, S. *Curr. Opin. Immunol.* **2005**, *17*, 18−24.
(15) Guermonprez, P.; Valladeau, J.; Zitvogel, L.; Thery, C.; Amigorena, S. *Annu. Rev. Immunol.* **2002**, *20*, 621−667.
(16) Stepanek, P. *Dynamic Light Scattering*; Brown, W., Ed.; Oxford University Press: New York, 1993; Chapter 4.
(17) Babak, V.; Boury, F. *Colloid Surf., A* **2004**, *243*, 33−42.
(18) Dubochet, J.; Adrian, M.; Chang, J. J.; Homo, J-C.; Lepault, J.; McDowall, A. W.; Schultz, P. *Q. Rev. Phys.* **1988**, *21*, 129−228.
(19) Harris, J. R. *Negative Staining and Cryoelectron Microscopy: The Thin Films Techniques*; Bios Scientific Publishers: Oxford, U.K., 1997.
(20) Negrete-Herrera, N.; Letoffe, J. M.; Putaux, J. L.; David, L.; Bourgeat-Lami, E. *Langmuir* **2004**, *20*, 1564−1571.
(21) Imberty, A.; Wimmerova, M.; Mitchell, E. P.; Gilboa-Garber, N. *Microb. Infect.* **2004**, *6*, 222−229.
(22) Lameignêre, E.; Imberty, A. Unpublished data, 2006.
(23) Dam, T. K.; Brewer, C. F. *Chem. Rev.* **2002**, *102*, 387−430.
(24) Thomson, J. A.; Ladbury, J. E. In *Biocalorimetry II. Applications of Calorimetry in the Biological Sciences*; Ladbury, J. E., Doyle, M. L., Eds.; J. Wiley & Sons, Ltd: Chichester, England, 2004; Chapter 2.
(25) Conchie, J.; Levvy, G. A. *Methods Carbohydr. Chem.* **1963**, *2*, 345−347.
(26) Duda, A.; Penczek, S. *Makromol. Chem. Macromol. Symp.* **1991**, *47*, 127−140.
(27) Vangeyte, P.; Jérôme, R. *J. Polym. Sci. Polym. Chem.* **2004**, *42*, 1132−1142.
(28) Detrembleur, C.; Mazza, M.; Lou, X.; Halleux, O.; Lecomte, P.; Mecerreyes, D.; Hedrick, J. L.; Jérôme, R. *Macromolecules* **2000**, *33*, 7751−7760.
(29) Detrembleur, C.; Mazza, M.; Halleux, O.; Lecomte, P.; Mecerreyes, D.; Hedrick, J. L.; Jérôme, R. *Macromolecules* **2000**, *33*, 14−18.
(30) Gautier, S.; D'Aloia, V.; Halleux, O.; Mazza, M.; Lecomte, P.; Jérôme, R. *J. Biomater. Sci., Polym. Ed.* **2003**, *14*, 63−85.
(31) Hazziza-Laskar, J.; Nurdin, N.; Helary, G.; Sauvet, G. *J. Appl. Polym. Sci.* **1993**, *50*, 651−662.
(32) Ybert, C.; Di Meglio, J.-M. *Langmuir* **1998**, *14*, 471−475.
(33) Beverung, C. J.; Radke, C. J.; Blanch, H. W. *Biophys. Chem.* **1998**, *70*, 121−132.
(34) Beverung, C. J.; Radke, C. J.; Blanch, H. W. *Biophys. Chem.* **1999**, *81*, 59−80.
(35) Yu, Y.; Eisenberg, A. *J. Am. Chem. Soc.* **1997**, *119*, 8383−8384.
(36) Vangeyte, P.; Gautier, S.; Jérôme, R. *Colloid Surf., A: Physicochem. Eng. Aspects* **2004**, *242*, 203−211.
(37) Jette, K. K.; Law, D.; Schmitt, E. A.; Kwon, G. S. *Pharm. Res.* **2004**, *21*, 1184−1191.
(38) Nagasaki, Y.; Okada, T.; Scholz, C.; Iijima, M.; Kato, M.; Kataoka, K. *Macromolecules* **1998**, *31*, 1473−1479.
(39) Mahmud, A.; Xiong, X.-B.; Lavasanifar, A. *Macromolecules* **2006**, *39*, 9419−9428.
(40) Dam, T. K.; Brewer, C. F. *Chem. Rev.* **2002**, *102*, 387−429.
(41) Pokorna, M.; Cioci, G.; Perret, S.; Rebuffet, E.; Kostlanova, N.; Adam, J.; Gilboa-Garber, N.; Mitchell, E. P.; Imberty, A.; Wimmerova, M. *Biochemistry* **2006**, *45*, 7501−7510.
(42) Charlot, A., Heyraud, A.; Guénot, P.; Rinaudo, M.; Auzély-Velty, R. *Biomacromolecules* **2006**, *7*, 907−913.
(43) Nagasaki, Y.; Yasugi, K.; Yamamoto, Y.; Harada, A.; Kataoka, K. *Biomacromolecules* **2001**, *2*, 1067−1070.
(44) Joralemon, M. J.; Murthy, K. S.; Remsen, E. E.; Becker, M. L.; Wooley, K. L. *Biomacromolecules* **2004**, *5*, 903−913.

BM070342Y